

Atomistic Simulation

[Introduction]

Atomistic simulations cover the other end of the length and time scale compared to the continuum (finite element) approach. They are used to calculate the behavior of single atoms (or molecules) and to study problems on a small scale, such as protein folding, the crystal structure of complex alloys, and crack propagation. Crystal structures have historically been used to classify and study the mechanical properties of materials. The fcc, hcp, and bcc metals, as well as diamond-cubic semiconductors, have all received significant attention and developed into prototypes for different types of mechanical behavior. In the present practical, we studied basic atomistic applications, like the computation of lattice and elastic constants for simple crystals, like copper, at 0 K and the simulation of bond breaking in a carbon nanotube.

In the last decades, copper has been a subject of study by many scientists and researchers, as it is not only an essential nutrient for the human body, which (together with iron) enables the body to form red blood cells and helps maintain healthy bones, blood vessels, nerves, and immune function, and it contributes to iron absorption, but at the same time, it can be used in daily life. Most copper is used in electrical equipment such as wiring and motors. This is because it conducts heat and electricity very well and can be drawn into wires. It also has uses in construction (for example, roofing and plumbing), and industrial machinery (such as heat exchangers). [1]

On the other hand, a carbon nanotube shows different important mechanical, electrical, and structural properties. Over the decades, they have been used for electronics, biosensing, and chemical sensing. They have large surface area that is why they are used as absorbents. Moreover, carbon nanotubes are used to remove heavy metals and organics from wastewater. The potential uses of carbon nanotubes are vast given their advantageous properties, such as having high levels of conductivity, a high melting point, and strong covalent bonds between their atoms. They can be single-walled, with diameters as little as 1 nanometer (nm), or multi-walled, measuring more than 100 nm in diameter. For this reason, scientists have explored how these structures can be taken advantage of. One field in which the use of carbon nanotubes has shown much promise is biomedical science. [3]

The focus is on the application and possible pitfalls rather than the numerics behind the scene. We used Lammmps, a simulation tool for particle-based materials modeling at the atomistic, meso, and continuum scales to obtain the most accurate possible results. Nonetheless, an understanding of numerics helps to interpret the obtained results. This sub-unit of molecular dynamics involves essential atomistic applications defined to be computations of lattice and elastic constants for simple crystals at 0K and equally involve the simulation of breaking the bond of carbon nanotube.

To attain the desired results then, three paramount quantities have to be defined.

- Initial configuration of the atom under consideration, its boundary conditions, and the quantities to be conserved,
- Potentials from which the forces are calculated,
- A numerical solver required to solve a dynamic system or a static system, i.e. the integration rule.

The above quantities, once defined accordingly, pave the way to successful simulations regarding the desired parameter.

Answer to Task 2.1: Part 1

Effective medium theory (EMT) is analytical or theoretical modeling technique that describes macroscopic properties of composite materials. The first model was developed by Faraday (1837). There is a wide variation in the values of the materials at the constituent level. So this fact makes it nearly impossible to calculate the many constituent values precisely. Theories, however, have been developed that can produce acceptable approximations, which in turn describe useful parameters, such

as the effective permittivity and permeability of the materials.

On the other hand the pair potential as illustrated by Lennard Jones (LJ) describes the potential energy of interaction between two non-bonding particles based on their distance of separation. This concept explains exhaustively on the forces behind the existence of the non-bonding particles at their respective positions. Through pair potential it is understood that particles at infinite distance don't interact and similarly for particle at a reasonably close to each other are bound to interact as the energy potential is within the responsive region of the potential energies.

However, we can not compare effective medium theory with Lennard-Jones, since the first one is a theory, and the other is a semi-empirical potential. So, for that reason, we will make a comparison between an EMT based potential, like EAM, and LJ.

So, let's start with Lennard-Jones potential. The mathematical form which described it is:

$$\phi(r_{ij}) = 4\epsilon_0 \left[\left(\frac{\sigma}{r_{ij}} \right)^{12} - \left(\frac{\sigma}{r_{ij}} \right)^6 \right] \quad (1)$$

where:

- the term with the power 12 represents atomic repulsion,
- the term with power 6 represents attractive interactions,
- the parameter σ is the distance at which the intermolecular potential between the two particles is zero. It gives a measurement of how close two nonbonding particles can get and is thus referred to as the van der Waals radius. It is equal to one-half of the internuclear distance between nonbonding particles ,
- the parameter ϵ_0 is the well depth and a measure of how strongly the two particles attract each other.

In opposition, the EAM potential is defined as:

$$U_i = \sum_{j=1}^{N_i} \phi(r_{ij}) + f(\rho_{ij}) \quad (2)$$

where:

- ρ_i is the local electron density which depends on the local environment of the atom i
- f the embedding function, which describes how the energy of an atom depends on the local energy density.

The potential features a contribution by a two-body term ϕ to capture the basic repulsion and attraction of the atoms, just like LJ, in conjunction with a multi-body term that accounts for the local electronic environment of the atom.

Moreover, pair potentials can predict too large dislocation loops, rapid partial expansion, and small cross slip, resulting in overestimating work hardening.

To sum up, as we can also in Fig.1, the EAM is a multi-body potential that can present different effective pair interactions between bonds at a surface and in the bulk.[1]

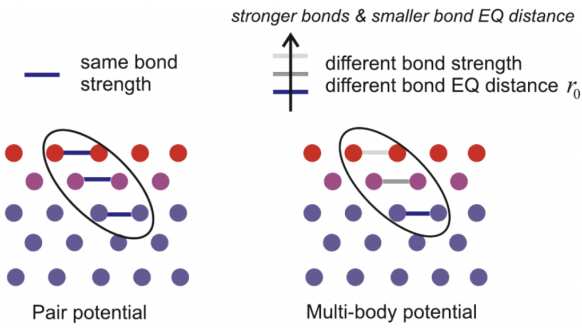


Figure 1: As we can see in the image here, there is a difference in the bond properties at the surface. Pair potentials are not able to define bonds in different environment, as all bonds are equal. To represent the change in bond properties of a surface , one needs to adapt a description that considers the environment of an atom to determine the bond strength, as it shown in the right panel. The bond energy between two particles is then no longer simply a function of its distance, but instead a function of the positions of all other particles in the vicinity. (This image is from the book " Atomistic Modeling of Materials Failure" by Markus J. Buehler, 2008, Springer Science+ Business Media,LLC)

Answer to Task 2.1: Part 2

First of all, as we know, the concept of the total energy of the system is simply a sum over the energy contribution between all pairs of the atoms in a system is a big simplification that leads to great challenges. For example, at a surface of a crystal, the atomic bonds may have different properties than in a bulk. Pair potentials, like LJ, are not capable of capturing this effect. Their limitation to model more complex situation,in particular the dependence of the properties of chemical bonds between pair of atoms is showing in the Fig.1. This behavior is very important for metals, because of quantum mechanical effects that describe the influence of the electron gas. Also, EAM potential is used to calculate the atomic action in the same material region, while LJ potential is used in the interface region of dissimilar materials. Finally, a pair potential may be based on theory (e. g. Coulomb), based partly on theory and partly on simple empirical assumptions (LJ, Buckingham) or may be based entirely on empirical functions. So, we cannot say that pair potentials are an opposite of empirical, semi-empirical or theoretical potentials.

Answer to Task 2.1: Part 3

As shown in the formula above, the EMT model has to rely on the electron density in a material, and can easily deduct bulk properties form that: The typically fitted parameters include equilibrium lattice constants, sublimation energy, bulk modulus, elastic constants, and vacancy-formation energy. Pair potentials typically fit lattice and elastic constants.

Answer to Task 2.1: Part 4

As it is mentioned in the theory, it is not necessary to investigate the parameters of copper, since we had to investigate only a simple copper lattice. So, there is no need to fit the parameters for the potential on our own. In LAMMPS software, we can set the formula(s) that LAMMPS uses to compute pairwise interactions. The pair potentials are defined between pairs of atoms that are within a cutoff distance and the set of active interactions typically changes over time.Also, we can use the bond_style command to define potentials between pairs of bonded atoms, which typically remain in place for the duration of a simulation.

Furthermore, in LAMMPS, pairwise force fields encompass a variety of interactions, some of which include many-body effects, e.g. EAM, Stillinger-Weber, Tersoff, REBO potentials. They are still classified as "pairwise" potentials because the set of interacting atoms changes with time (unlike molecular bonds) and thus a neighbor list is used to find nearby interacting atoms.

Moreover, the coefficients associated with a pair style are typically set for each pair of atom types, and are specified by the pair_coeff command or read from a file by the read_data or read_restart

commands.

The pair_modify command sets options for mixing of type I-J interaction coefficients and adding energy offsets or tail corrections to Lennard-Jones potentials. Details on these options as they pertain to individual potentials are described on the doc page for the potential. Likewise, info on whether the potential information is stored in a restart file is listed on the potential doc page.

In many cases, the global cutoff value can be overridden for a specific pair of atom types by the pair_coeff command.

In our case with the copper, we used EAM as forced field and we used the Cu_zhou.eam.alloy as interatomic potential files from Gitlab.[4]

Additionally, as stated in the introduction above, copper has been the subject of research for decades. With simple internet browsing, we found some indicative values of lattice constants [5] together with the corresponding energies listed in table 1 below.

Lattice constant (\AA)	Energy (eV)
3.15	-9528.0714
3.46	-13769.586
3.75	-13935.203

Table 1: Experimental lattice constants extracted by different papers and their energies.

Answer to Task 3.1

a) The Face-Centered Cubic (FCC) unit cell can be imagined as a cube with an atom on each corner, and an atom on each face, as we can see in the Fig.2. It is one of the most common structures for metals. FCC has 4 atoms per unit cell, lattice constant $a = 2R\sqrt{2}$, where R is the atomic radius. In the case of the closed plane the atoms are assumed to touch along the diagonals of the faces on each face of the cube.[6]

In our case for example, if we consider the atomic radius to be $R = 128 = pm = 1.28\text{\AA}$, then the lattice constant $a = 362pm = 3.62\text{\AA}$.

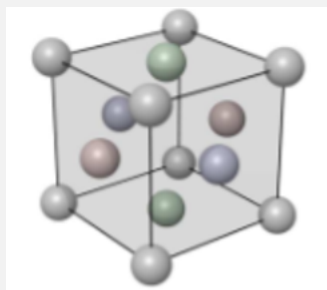


Figure 2: The FCC structure (Atoms=Face Centered Cubic(size=3,3,3), symbol="Cu",PBC=True)

b) The Body-Centered Cubic (BCC) unit cell can be imagined as a cube with an atom on each corner, and an atom in the cube's center. It is one of the most common structures for metals. Its structure is as shown in the Fig.3. BCC has 2 atoms per unit cell, lattice constant $a = 4R/\sqrt{3}$, where R is the atomic radius. In the case of the close Packed Plane cuts the unit cube in half diagonally.[7] Again as we saw above for FCC crystal structure, in our case we consider that the atomic radius is $R = 128 = pm = 1.28\text{\AA}$, then the lattice constant $a = 295pm = 2.95\text{\AA}$.

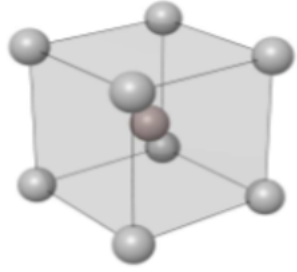


Figure 3: The BCC structure (Atoms=Body Centered Cubic(size=3,3,3), symbol="Cu",PBC=True)

Answer to Task 3.2

We used Lammmps Software to calculate the minimal energies W at $0K$ in a molecular statics simulation for the three cubic crystal structures. We used the estimated lattice constants, as are shown in the Table 2, as a starting parameter and we tried to vary them to find the structure and the lattice constant l_0 with the smallest potential energy.

Crystal Structure	Lattice constant (\AA)
fcc	3.621
bcc	2.956
scc	2.567

Table 2: The three cubic crystal structures and their estimated lattice constants.

The plot of the results in an energy lattice constant plot conforming to the equation $W = p_0 + p_1 l + p_2 l^2$. The results imply that the lattice constant, l is the coefficient of the said function and therefore the W_0 is the l axis intercept when the plot is the origin.

So, we took three cases of cubic crystals structures, which are the following:

- fcc, with $l = 3.621 \text{ \AA}$ and we found out that the $W = -14153.32 \text{ eV}$. Also, we can see the fcc structure using the VMD program in Fig.4.

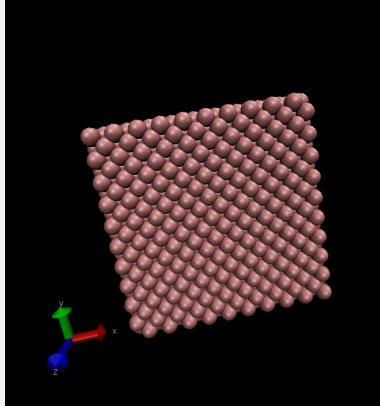


Figure 4: The fcc crystal structure via VMD program.

- bcc, with $l = 2.956 \text{ \AA}$ and we found out that the $W = -6926.54 \text{ eV}$. Also, we can see the bcc structure using the VMD program in Fig.5.

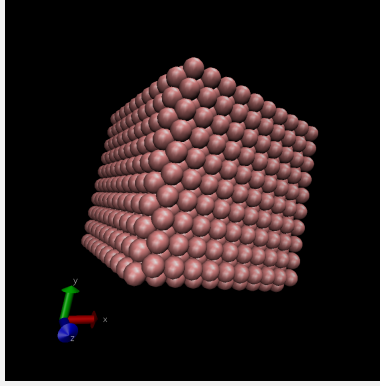


Figure 5: The bcc crystal structure via VMD program.

- scc, with $l = 2.567 \text{ \AA}$ and we found out that the $W = -2098.2494 \text{ eV}$. Also, we can see the scc structure using the VMD program in Fig.6.

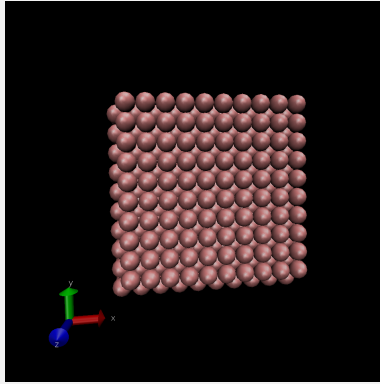


Figure 6: The scc crystal structure via VMD program.

From the results that we received and as we can see in the table 3, we can assume that for the bcc and scc crystal structures, the energy is much larger than the fcc. At this point we have to mention that in Lammps software the energy's unit is eV.

Crystal Structure	Lattice constant (\AA)	Total Energy (eV)
fcc	3.621	-14158.838
bcc	2.956	-6867.9498
scc	2.567	-3035.1401

Table 3: The results of the total energies for the three cubic crystal structures and their estimated lattice constants.

Furthermore, we plot the results in an energy-lattice constant plot, and fit the data to a second order polynomial ($W = p_0 + p_1 l + p_2 l^2$) with the coefficients p_0, p_1, p_2 .

To do that we solve the polynomial for the energy minimum, $\min\{W\} = W_0$, and give the results (l, W_0) for the three lattices. Below, we can see in Figs.7,8,9 the energy lattice plots for the three crystal structures that we have. Moreover, in the tables 4,5 and 6 we can see the data that we used and were calculated by Lammps software.

By given the seven points for each crystal structure and using Python program, we got the following results:

Lattice constant (\AA)	Total Energy (eV)
2.367	-72639.632
2.997	-4412.381
3.125	-8870.7905
3.621	-14158.838
3.988	-12815.233
4.367	-10408.056
4.997	-6144.0533

Table 4: The lattice constants together with the corresponding energies the fcc crystal structure, calculated with the program Lammps.

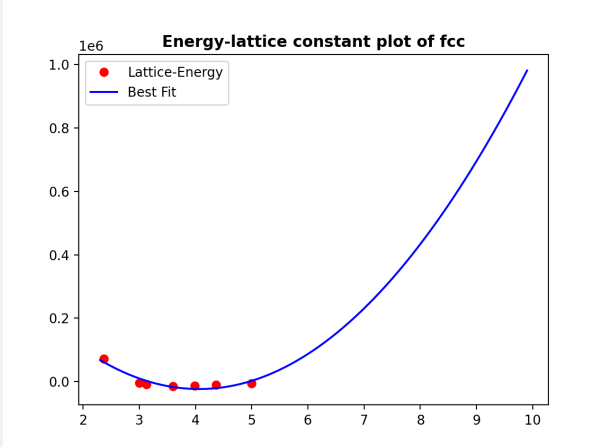


Figure 7: The energy-lattice constant plot of fcc with the data from the Table 3.

Lattice constant (\AA)	Total Energy (eV)
2.067	14200.642
2.367	-1816.8076
2.467	-4174.6372
2.656	-5519.6794
2.874	-5722.8194
2.956	-6867.9498
3.067	-6686.8232

Table 5: The lattice constants together with the corresponding energies the bcc crystal structure, calculated with the program Lammps.

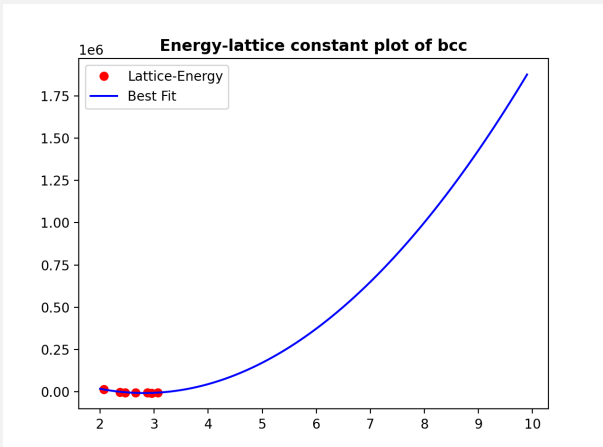


Figure 8: The energy-lattice constant plot of bcc with the data from the Table 4.

Lattice constant (\AA)	Total Energy (eV)
1.467	13841.844
1.967	-1246.248
2.067	-2255.2312
2.227	-2989.8638
2.367	-3153.6773
2.467	-3138.5226
2.567	-3035.1401

Table 6: The lattice constants together with the corresponding energies the scc crystal structure, calculated with the program Lammps.

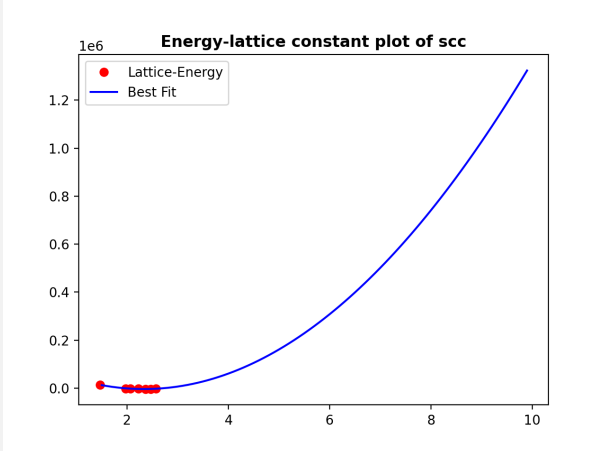


Figure 9: The energy-lattice constant plot of scc with the data from the Table 5.

As we can see from the above diagrams 7,8,9, as well as from the values recorded in tables 4,5,6, we conclude that as we increase the value of the parameter, the value of the temperature also increases. However, we observe that as far as the results of the fcc crystal structure are concerned, the temperature does not vary so much. More specifically, from the plot of the lattice parameter dependent total energy (Fig. 7), the most stable structure is found to be FCC in agreement with experiment.

Answer to Task 3.3

Elastic constant describes the mechanical behavior of a material and its possible strain distribution can be computed for through numerous substitutions of parameters involved.

Voigt notation is useful to understand the 4th-rank tensors of geophysics, for example the elastic stiffness tensor $\{C_{ijkl}\}$, needed for wave propagation, or the elastic compliance tensor $\{S_{ijkl}\}$, needed for geomechanics. These tensors are hard to understand intuitively, since one cannot write them down on paper. (If you use i to index the rows, and j to index the columns, where do you put the indices k and l ?).

But, Woldemar Voigt (1850-1919) realized that because stress and strain are symmetric tensors, and because the order of the index pairs ij and kl can be interchanged, all the information in these 4th-rank tensors is contained in symmetric 2nd-rank matrices (which can be written on paper!).

This transform, called Voigt notation, should be used for displays (to aid intuition), not for calculation, since the matrices do not obey tensor algebra.[8]

As we saw in the theory the stiffness tensor is the second derivative of the strain energy density with respect to ϵ :

$$C = \frac{\partial^2 W^e}{\partial \epsilon^2} \quad (3)$$

Also we can write the strain energy density as:

$$W^e = \frac{1}{2} : \epsilon \cdot C \cdot \epsilon \quad (4)$$

Also, Voigt notation is the standard mapping for tensor indices and taking advantage of the mirroring effect, we have:

$i,j \rightarrow \alpha$
 $11 \rightarrow 1$
 $22 \rightarrow 2$
 $33 \rightarrow 3$
 $23,32 \rightarrow 4$
 $13,31 \rightarrow 5$
 $12,21 \rightarrow 6$

$$\begin{bmatrix} \epsilon_{11} \\ \epsilon_{22} \\ \epsilon_{33} \\ 2\epsilon_{23} \\ 2\epsilon_{13} \\ 2\epsilon_{12} \end{bmatrix} = \begin{bmatrix} \epsilon_1 \\ \epsilon_2 \\ \epsilon_3 \\ \epsilon_4 \\ \epsilon_5 \\ \epsilon_6 \end{bmatrix} \quad (5)$$

In the case of a linear elastic isotropic behavior, there are only two independent coefficients and we have the following stiffness matrix.

$$C_{iso}^\nu = \begin{bmatrix} C_{11} & C_{12} & C_{12} & 0 & 0 & 0 \\ C_{12} & C_{11} & C_{12} & 0 & 0 & 0 \\ C_{12} & C_{12} & C_{11} & 0 & 0 & 0 \\ 0 & 0 & 0 & \frac{C_{11}-C_{12}}{2} & 0 & 0 \\ 0 & 0 & 0 & 0 & \frac{C_{11}-C_{12}}{2} & 0 \\ 0 & 0 & 0 & 0 & 0 & \frac{C_{11}-C_{12}}{2} \end{bmatrix} \begin{bmatrix} \epsilon_{11} \\ \epsilon_{22} \\ \epsilon_{33} \\ 2\epsilon_{23} \\ 2\epsilon_{13} \\ 2\epsilon_{12} \end{bmatrix} \quad (6)$$

Now, if we would like to write the second-order elastic tensor denoted C , relating the stress tensor to the strain tensor as is shown in the eq.7 of the theory script, we will use a combination of eq.3,4, and 5. So, in the end we can write that:

$$C_{12} = \frac{2W^e}{\bar{\epsilon}_2 \bar{\epsilon}_2} \quad (\text{the same applies respectively to } \epsilon_1 \text{ and } \epsilon_3) \quad (7)$$

or

$$C_{12} = C_{11} - \frac{4W^e}{\bar{\epsilon}_6 \bar{\epsilon}_6} \quad (\text{the same applies respectively to } \epsilon_4 \text{ and } \epsilon_5) \quad (8)$$

Answer to Task 3.4

In cubic crystals when the axis system is parallel to the crystal axes, there are only three independent elastic constants: $c_{11} = c_{22} = c_{33}$, $c_{12} = c_{23} = c_{31}$ and $c_{44} = c_{55} = c_{66}$, written conventionally as c11, c12 and c44.

In the case of a linear elastic isotropic behavior, we have the following stiffness matrix.

$$C_{ortho}^v = \begin{bmatrix} C_{11} & C_{12} & C_{12} & 0 & 0 & 0 \\ C_{12} & C_{11} & C_{12} & 0 & 0 & 0 \\ C_{12} & C_{12} & C_{11} & 0 & 0 & 0 \\ 0 & 0 & 0 & C_{44} & 0 & 0 \\ 0 & 0 & 0 & 0 & C_{44} & 0 \\ 0 & 0 & 0 & 0 & 0 & C_{44} \end{bmatrix} \begin{bmatrix} \epsilon_{11} \\ \epsilon_{22} \\ \epsilon_{33} \\ 2\epsilon_{23} \\ 2\epsilon_{13} \\ 2\epsilon_{12} \end{bmatrix} \quad (9)$$

Again, if we would like to write the second-order elastic tensor denoted C , relating the stress tensor to the strain tensor as is shown in the eq.7 of the theory script, we will follow the same strategy like above in task 3.3. So, we will get :

$$C_{44} = \frac{2W^e}{\bar{\epsilon}_4 \bar{\epsilon}_4} \text{(the same applies respectively to } \epsilon_5 \text{ and } \epsilon_6) \quad (10)$$

Answer to Task 3.5

In this task we have to evaluate the elastic constants of copper in the fcc configuration. As we know, cubic crystal lattices usually have a orthotropic symmetry, so that we can use the deformation states from task 3.3. First of all, we start with the optimal lattice parameter l from task 3.2 for fcc. Then, we have to relax the structure by applying minimization. Then, we have to deform the structure with the strains that you have identified in task 3.3 and task 3.4 to calculate the elastic constants from the elastic energy density. We can do all these calculations easily in lammps without using the third polynomial by exchanging the structure for fcc copper (init.mod) and the potential (potential.mode file) for an EAM potential of copper. So as we can see in the table 7, we printed the full stiffness tensor already without any need for polynomial fitting. Otherwise, we wrote down only the elastic constants C_{11} , C_{12} , C_{44} in the table 7, so it will be easier to compare it with the values of Table 1 in the theory. Also, because the units of elastic constant in lammps are given in GPa, we converted them in N/m^2 .

Elastic constants	Experimental Value ($10^{11} N/m^2$)	Theoretical Value ($10^{11} N/m^2$)
C_{11}	1.8041	1.7620
C_{12}	1.1710	1.2494
C_{44}	0.7065	0.8177

Table 7: Single-crystal elastic constants in $10^{11} N/m^2$ of copper at $T=OK$.

As we can observe, there is not much difference in the values with the error (in percentage) for each elastic constant C_{11} , C_{12} , C_{44} respectively shown in Table 8. As we can see it is in total less than 15%.

Experimental Value ($10^{11} N/m^2$)	Theoretical Value ($10^{11} N/m^2$)	Percent Error (%)
1.8041	1.7620	2.38933
1.1710	1.2494	6.27501
0.7065	0.8177	13.5991

Table 8: The error (in percent) for each constant.

Answer to Task 3.6

By looking at the strain energy plots, we can give an approximate of the range around the relaxed state for which this assumption is reasonable. Moreover, by looking the plots, we can notice that as the temperature T increases, it affects the strain-energy plot. The blue line in Figs.10-14 represents the Young's module. Also, we can assume that the elastic regime appears in the first few points.

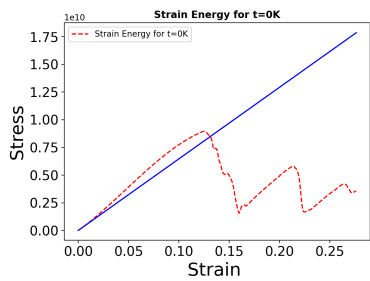


Figure 10: The stress-strain plot for T=0K.

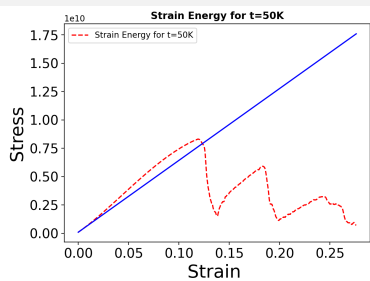


Figure 11: The stress-strain plot for T=50K.

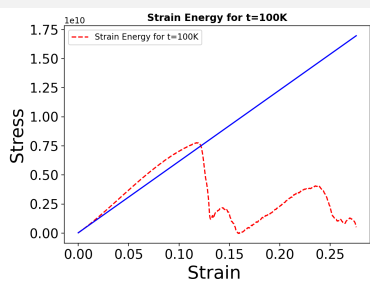


Figure 12: The stress-strain plot for T=100K.

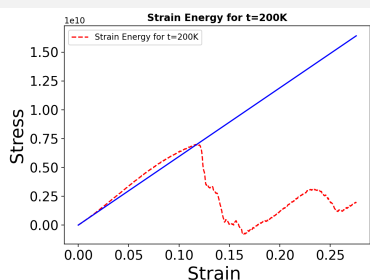


Figure 13: The stress-strain plot for T=200K.

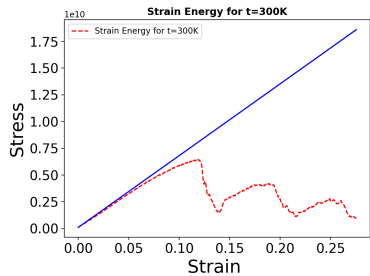


Figure 14: The stress-strain plot for T=300K.

Answer to Task 4.1

Under this task the CNT type under consideration will be 5,5 nanotube (armchair nanotube) but before then besides this type there exists other two types of nanotubes. These are:

1. Zigzag carbon nanotubes
2. Chiral carbon nanotubes
3. Armchair nanotube

These types of CNT nanotubes are as a result of the graphite being rolled up and consequently amounting to the three varied types.

Under this tasks the 5,5 nanotube (see Fig. 15) also referred to as armchair nanotube if found to exhibit numeral mechanical behaviors with most outstanding being:

1. High thermal and electrical conductivity, this is due to the nature of graphite material used,
2. Aspect ratio which defines a number of physical properties,
3. High elasticity. This property is mostly derived from the nature of amorphous existence of carbon and specifically the graphite form,
4. High tensile strength as exhibit by the nature of carbon atom,
5. Highly flexible and with low thermal expansion coefficient.[9]

These define the mechanical behavior of the 5,5 nanotube.

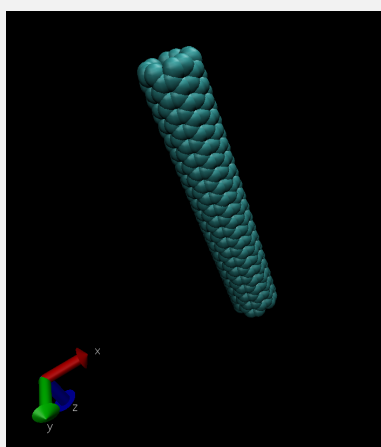


Figure 15: The 5,5 nanotube via VMD program.

Answer to Task 4.2

In a first step we wanted to estimate a critical deformation rate, in which the system has not enough time to relax and therefore is unstable.

For that purpose, we simulate a stretching of the nanotube along the longitudinal axis in a NVE ensemble. Also, the velocity-verlet algorithm for the integration was used.

Start with the relaxed state at $0K$, and incrementally deform the system. Then, we chose a small time step, $0.1fs$ and investigate the relaxation time.

After that, we chose a different time step $1fs$ (in the Lammps script, we wrote $0.001ps$). Also, we tried to estimate the critical deformation rate for which the system becomes unstable.

We ended up that for a given deformation rate is it better to have many small steps with short relaxations because for larger steps, the system is going to "break". The output of the Lammps programs are shown in the Figs.16 and 17.

```
Loop time of 80.7385 on 4 procs for 150000 steps with 420 atoms
Performance: 16.052 ns/day, 1.495 hours/ns, 1867.849 timesteps/s
99.6% CPU use with 4 MPI tasks x 1 OpenMP threads

MPI task timing breakdown:
Section | min time | avg time | max time | %varavg| %total
-----+-----+-----+-----+-----+
Pair | 57.244 | 66.165 | 74.84 | 106.2 | 81.95
Bond | 0.0048622 | 0.0049448 | 0.0050503 | 0.1 | 0.01
Neigh | 0.00066279 | 0.00066845 | 0.00067612 | 0.0 | 0.00
Comm | 5.3731 | 14.036 | 22.973 | 230.6 | 17.38
Output | 0.033086 | 0.036942 | 0.048432 | 3.5 | 0.05
Modify | 0.23411 | 0.25123 | 0.2667 | 2.8 | 0.31
Other | 0.2443 | | | | 0.30

Nlocal:          105 ave      115 max      96 min
Histogram: 2 0 0 0 0 0 0 0 1 1
Nghost:           485 ave      494 max     475 min
Histogram: 1 1 0 0 0 0 0 0 0 2
Neighs:            0 ave       0 max       0 min
Histogram: 4 0 0 0 0 0 0 0 0 0
FullNghs:        15775.5 ave    17289 max   14401 min
Histogram: 2 0 0 0 0 0 0 0 1 1

Total # of neighbors = 63102
Ave neights/atom = 150.24286
Ave special neights/atom = 0
Neighbor list builds = 1
Dangerous builds = 0
Total wall time: 0:01:22
```

Figure 16:Here is the results for small tome step $0.1fs$

```

Loop time of 2.21915 on 4 procs for 5000 steps with 420 atoms

Performance: 194.670 ns/day, 0.123 hours/ns, 2253.120 timesteps/s
99.4% CPU use with 4 MPI tasks x 1 OpenMP threads

MPI task timing breakdown:
Section | min time | avg time | max time | %varavg| %total
-----
Pair   | 1.3697  | 1.7185  | 2.0794  | 19.3  | 77.44
Bond   | 0.00015169 | 0.00015729 | 0.00016468 | 0.0  | 0.01
Neigh   | 0         | 0         | 0         | 0.0  | 0.00
Comm   | 0.12017  | 0.48063  | 0.82878  | 36.4  | 21.66
Output  | 0.0012408 | 0.0013961 | 0.0018551 | 0.7  | 0.06
Modify  | 0.0074884 | 0.0085434 | 0.0096881 | 0.9  | 0.38
Other   |           | 0.00991  |           |       | 0.45

Nlocal:          105 ave      126 max      84 min
Histogram: 1 0 0 0 0 2 0 0 0 1
Nghost:          495 ave      516 max     474 min
Histogram: 1 0 0 0 0 2 0 0 0 1
Neighs:          0 ave       0 max       0 min
Histogram: 4 0 0 0 0 0 0 0 0 0
FullNghs:        15645 ave    18774 max    12516 min
Histogram: 1 0 0 0 0 2 0 0 0 1

Total # of neighbors = 62580
Ave neights/atom = 149
Ave special neights/atom = 0
Neighbor list builds = 0
Dangerous builds = 0
Total wall time: 0:00:02

```

Figure 17: Here is the results for small tome step 1*fs*.

Answer to Task 4.3

Using the Lammmps software, we plotted the kinetic, potential and total energy (see Figs.18,19 and 20) of the system at $0K$.

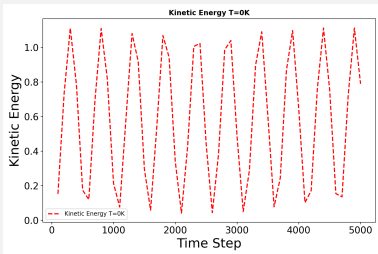


Figure 18: The kinetic energy of the system at $T=0K$.

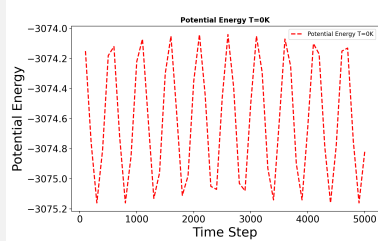


Figure 19: The potential energy of the system at $T=0K$.

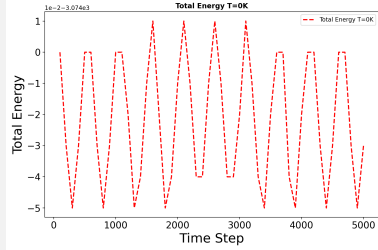


Figure 20: The total energy of the system at $T=0K$.

Answer to Task 4.4

In application of the NVT ensemble the uniaxial deformation at $T = 300K$.

From the observation then the energy at $T = 300K$ shows a strong correlation between the temperature rise hence increase in temperature causes a decline in energy required to deform the nanotube as the atoms are excited and deformity requires less energy as compared to less excited particles as witnessed in the 5,5 nanotube (armchair nanotube). The results of the three different energies at $T=300K$, kinetic, potential and total are shown in the corresponding Figs.21,22 and 23.

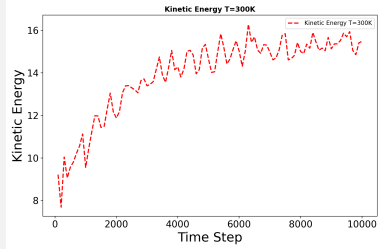


Figure 21: The kinetic energy of the system at $T=300K$.

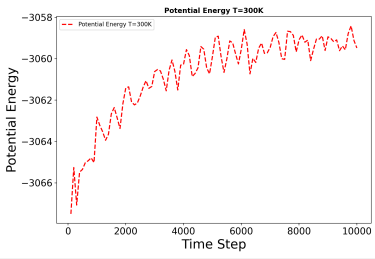


Figure 21: The potential energy of the system at T=300K.

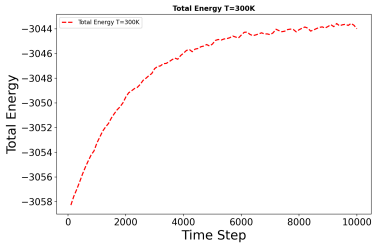


Figure 22: The total energy of the system at T=300K.

Answer to Task 4.5

On obtaining a stress strain curve from the calculations then a numerous cases are to be considered for both stress and strain computation and the corresponding values are to be plotted as shown below in the Fig.23.

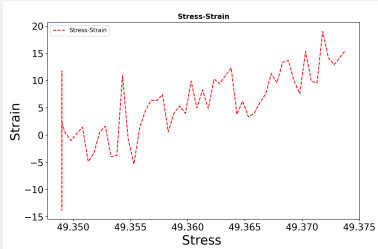


Figure 23: The stress-strain plot at T=293K.

1 References

[1] Health benefits and risks of copper

<https://www.medicalnewstoday.com/articles/288165>

[2] The Importance of Carbon Nanotube Surface Roughness

<https://wwwazonano.com/article.aspx?ArticleID=5701>

[3] Markus J. Buehler (2008), "Atomistic Modeling of Materials Failure ", Springer.

[4] potentials/Cu_zhou.eam.alloy·master·exaalt/lammps·GitLab

https://gitlab.com/exaalt/lammps/-/blob/master/potentials/Cu_zhou.eam.alloy

[5] Personales.unican.es

https://personales.unican.es/junqueraj/JavierJunquera_files/Metodos/Structuralproperties/Lattice-constant-si/Exercise-structure-si.pdf

[6] Body-Centered Cubic (BCC) Unit Cell — Materials Science Engineering Student

<https://msestudent.com/body-centered-cubic-bcc-unit-cell/>

[7] Face-Centered Cubic (FCC) Unit Cell — Materials Science Engineering Student

<https://msestudent.com/face-centered-cubic-fcc-unit-cell/>

[8] Voigt notation - SEG Wiki

https://wiki.seg.org/wiki/Voigt_notation

[9] Carbon nanotube - Wikipedia

https://en.wikipedia.org/wiki/Carbon_nanotube

[10] Sandia National Laboratories (2003), "LAMMPS Users Manual, Large-scale Atomic/Molecular Massively Parallel Simulator", <http://lammps.sandia.gov>, Sandia Corporation.

[11] Releases · lammps/lammps

<https://github.com/lammps/lammps/releases>